Snow Depth Distribution Mapping in a Post-fire Landscape from UAS LiDAR

by

Devlin Alexander Rutherford

A thesis accepted and approved in partial fulfillment of the

requirements for the degree of

Master of Science

in Geography

Thesis Committee:

Jonathan C. Ryan, Chair

Sarah Cooley, Co-Chair

University of Oregon

Spring 2024

THESIS ABSTRACT

Devlin Alexander Rutherford

Master of Science in Geography

Title: Snow Depth Distribution Mapping in a Post-fire Landscape from UAS LiDAR

Quantifying winter snowpack dynamics is crucial for forecasting water resources in the Western US where a large amount of snowmelt is impounded in artificial reservoirs. It is well known that snow accumulation and ablation processes are substantially modified by forest canopies. Disturbances to forests, such as wildfire and timber extraction, are therefore likely to have an important impact on snowpacks. However, few studies have investigated the extent to which wildfire impacts snow, especially in the PNW where forests have complex effects on snow. To address this need, we deployed an uncrewed aircraft system (UAS) equipped with a Light Detection and Ranging (LiDAR) sensor to map snow depth in a headwater catchment of Oregon's North Santiam River. In 2023, we surveyed a ~0.5 km^2 area covering both north and south aspects that exhibited variable forest density and burn severity. Over three surveys, we collected snow depth data on dates before, near and after peak snowpack depths, allowing us to examine periods of both snow accumulation and ablation. We observed consistently higher snow depths in open and severely burned forested areas compared to low and moderately burned forested areas for all surveys on both north and south aspects. The observed differences in snow depth persisted into the ablation season until much of the south facing forested area with low burn severity was snow-free. Our findings indicate that severe wildfire likely enhanced snow retention at our field site by reducing interception without significantly enhancing snow ablation. We conclude that wildfire has the potential to substantially modify snowpacks in maritime climates which has implications for management of water resources in the PNW.

ACKNOWLEDGMENTS

I wish to express my appreciation to Professors Ryan and Cooley for their assistance in the preparation of this manuscript. In addition, special thanks are due to my collaborators at Portland State University: Professor Kelly Gleason and her graduate students Sage Ebel and Siobhan (Nani) Ciafone, without whom this research could not have been completed. I also thank James Lamping and the members of the Cryo-Hydro lab group for their valuable input.

DEDICATION

I dedicate this manuscript to my parents, Gary, and Donna Rutherford.

Chapter Page

LIST OF FIGURES

LIST OF TABLES

1 INTRODUCTION

Snow is an important natural reservoir that, when melted, provides downstream communities with water for sanitation, crop irrigation, and power during dry seasons (Barnett et al., 2005; Mankin et al., 2015). In the western United States, a large amount of snowmelt is impounded in artificial reservoirs (Li et al., 2017). Managing water in the western United States therefore depends on accurate knowledge of water storage in snowpacks (i.e. snow water-equivalent or SWE). Producing operational forecasts of SWE depends on accurate understanding of the processes by which snow accumulates and ablates. Given that most high-elevation regions of the western US where snow accumulates are also forested (Rutter et al., 2009), understanding the response of snowpack dynamics to the presence of trees is therefore crucial.

Forests alter both the accumulation and ablation of snow in several ways. Forests reduce snow accumulation at the ground surface through interception (Hedstrom and Pomeroy, 1998; Winkler et al., 2005). Given that snow intercepted by tree canopy structure is well-ventilated, it is primed for sublimation, evaporation, and melt (Pomeroy and Schmidt, 1993; Storck et al., 2002). Due to these processes, a substantial portion of intercepted snow may never reach the forest floor (Lumbrazo et al., 2022). Forests in Saskatchewan, Canada and have been found to intercept and subsequently sublimate 25-45% of snowfall (Hedstrom and Pomeroy, 1998). Forests modify radiative and turbulent heat fluxes with consequences for snow ablation. Snow beneath forest canopies generally receives less solar radiation than adjacent open areas due to shading effects (Lawler and Link, 2011; Malle et al., 2019). On the other hand, snow beneath forest canopies receives more longwave radiation than adjacent open areas due to absorption and emittance of heat by tree trunks and branches (Malle et al., 2019; Sicart et al., 2004). Finally, forests reduce sensible heat fluxes by reducing wind speed (Trujillo et al., 2009).

The specific impacts of forests on snow accumulation and ablation depend on forest structure and climate (Lundquist et al., 2013; Roth and Nolin, 2017). Previous studies have found higher snow depths in tree canopy gaps because these areas are less impacted by interception but still experience shortwave radiation shading and attenuated wind speeds (Mazzotti et al., 2019). Studies of this kind have concluded that, in some areas, reducing forest density will result in an increase in water quantity (Dickerson-Lange et al., 2023). During cold winter temperatures in Colorado, wind redistribution of snow can result in significant differences between windward and leeward snow depths at forest edges (Currier and Lundquist, 2018). Wind driven snow redistribution past the forest edge and in topographic depressions has been observed in field-forest environments in Quebec, Canada (Dharmadasa et al., 2023). Comparisons between the forest-snow interactions must therefore consider the specific climatic and ecological setting in which snow measurements were collected.

The balance of processes controlling snow accumulation and ablation in forests is further complicated by canopy disturbances. For example, tree death from insect infestation and timber harvest has the potential to modify snowpacks by reducing canopy cover. Decreased snow interception rates and higher winter snowpack sublimation were observed in mountain pine beetle-killed forest stands (Biederman et al., 2014). Similarly, timber harvest can result in decreased snow interception and a shift to earlier snowmelt timing (Zhao et al., 2021). In the western United States, wildfires are responsible for large forest disturbances (Iglesias et al., 2022). Most studies find that more snow can accumulate in burned forests compared to nearby unburned forests (from 7% to 58%) due to reduced snow interception (Burles, 2011; Gleason et al., 2013; McGrath et al., 2023; Skidmore, 1994; Winkler, 2011).

The degree to which fire impacts forest canopy can vary across a landscape due to fuels, topography and fire suppression, resulting in a mosaic of burn severities (Koshkin et al., 2022). High severity burn removes forest canopy, moderate severity burn removes a portion of the forest canopy, and low severity burn only involves the combustion of surface fuels, leaving the forest canopy intact. A reduction in canopy density reduces the capacity of the burned forest to shade the snowpack from incoming solar radiation and shelter it from turbulent fluxes (Harpold et al., 2014). Additionally, in burned forest areas, black carbon and burned woody debris (BWD) concentrate on the snow surface and can decrease snow surface albedo and accelerate the growth of snow grains (Gleason et al., 2013; Painter et al., 2012; Skiles et al., 2018). The combination of reduced shading, reduced snow surface albedo, and increased exposure to wind has been demonstrated to enhance ablation rates in burned forests, especially in the later part of the melt season, relative to unburned forests (Skidmore, 1994; Gleason et al., 2019, 2013; Gleason and Nolin, 2016; Maxwell et al., 2019; McGrath et al., 2023). SWE losses attributed to mid-winter melt and sublimation losses has been shown to decrease peak SWE in burned forests (Harpold et al., 2014; McGrath et al., 2023). Decreased peak SWE and increased ablation rates result in earlier snow disappearance dates in burned forests relative to nearby unburned forests (Gleason et al., 2019, 2013; Gleason and Nolin, 2016; Maxwell et al., 2019; McGrath et al., 2023).

Most studies that have investigated the effects of wildfire on snowpacks have been conducted in continental climates with cold winters (e.g. Skidmore, 1994; Burles et al., 2011; Harpold et al., 2014; Gleason et al., 2019; Maxwell et al., 2019; McGrath et al., 2023). In these climates, where shortwave radiation is the dominant term in the surface energy balance, ablation rates are known to be lower in forests relative to open areas due to canopy shading effects (Lundquist et al., 2013). Therefore, it is not surprising that the removal of canopy cover by wildfire, combined with enhanced black carbon deposition, enhances ablation rates in burned forests relative to unburned forests. However, in maritime climates, such as the PNW, where longwave contributions have been shown to be the dominant component of the annual energy balance (Roth and Nolin, 2017), the effects of wildfire are likely to be more complex.

Finally, rates of snow accumulation and ablation in burned vs. unburned forests are likely to be modified by topography (i.e. elevation, slope, and aspect). Harpold et al. (2014), for example, identified that aspect became a more important control on winter season SWE following a wildfire due to the removal of canopy effects. Despite this, previous studies into wildfire effects on snow have focused on a relatively narrow range of topographies (Table 1). Almost all study sites sampled snow on flat terrain or on gentle (<18°) north-facing slopes. This is partly because these studies measured snow using ground-based techniques which are challenging to collect on steep slopes across large spatial scales. The effects of wildfire on snowpack dynamics are therefore less well known for steeper slope angles and south-facing aspects. Given that wildfire is increasing in size and severity in the Western United States (Marlon et al., 2012; Westerling et al., 2006), and the pronounced shift of wildfires from the intermittent snow zone into the seasonal snow zone (Kampf et al., 2022), understanding not only the effects of wildfire on snowpack dynamics, but also how this response varies with gradients in topography, slope and aspect, are therefore important for accurate projections of SWE at watershed scales and beyond.

The emergence of airborne LiDAR technology has made it possible to map snow depth distributions across large spatial scales, across a range of slopes, and beneath dense forest canopies. To do this, LiDAR surveys are completed in snow-free and snow-covered conditions. A snow depth model is generated by subtracting a snow-free digital elevation model from a snow-covered digital elevation model. Airborne LiDAR systems have demonstrated capability to reliably capture high resolution spatial snow distribution patterns in forested areas (Deems et al., 2013; Mazzotti et al., 2019). Airborne LiDAR has a long history of measuring snow depths, with programs such as NASA JPL's Airborne Snow Observatory (ASO) in existence since 2013. Airborne LiDAR data, while detailed, does not provide high enough data to resolve microscale process such as snow-vegetation interactions (Harder et al., 2016).

Author	Location	Study Sites	Elevation	Slope	Aspect	Peak SWE Δ	Ablation rate
Skidmore 1994	Southwest Montana	BF, UF, CC	2003m	0°	NA	+7% in BF. 0% vs. CC.	+57% (both BF and CC vs. UF)
Burles 2011	Southeast Alberta	BF, UF	1775m (BF), 1680m (UF)	4°-8°	NNE 45° (BF) NNW 340° (UF)	+50% (2009), +58% (2010) in BF.	+18 % (2009), +22 % (2010)
Winkler 2011	Southern British Colombia	BF, UF, CC. (5km apart)	1250m-1300m	0°	NA	+25% in BF. -21% vs. CC	+38% 1.46 cm/d in BF, .91 cm/d in UF.
Gleason 2013	Oregon Cascades	BF, UF	1750m	0°	NA	+11% in BF.	+63% 2.3 cm/d in BF, 1.2 cm/d in UF
Harpold 2014	Northern New Mexico	BF, UF	2700m-2800m	15°-18°	Multiple, largely N facing	-10% in BF.	Significantly more ablation in post-burn area
Maxwell 2019	Central Utah	BF, UF (N and S)	2900-3100m	15°	N an S	No change.	+0.9 cm/d for S aspect, +0.33 cm/d for N aspect
Smoot and Gleason 2021	Western USA (geospatial analysis)	SNOTEL sites in burn perimeters	Varies	Varies	Varies	50 yr. trend: −3.07 mm/yr. (All sites) −5.72 mm/yr. (Cascades)	+.3 cm/d. (10-year mean) in high severity burn. No sig. Δ across all sites
McGrath 2023	Northern Colorado	BF, UF, Open (SNOTEL)	3020m - 3096m	4°-5°	SE, NW	+14% in BF, 17% decrease v. SNOTEL	+144% vs. UF, +82% vs. SNOTEL

Table 1. Summary of previous snowpack studies in wildfire burn scars. Adapted and updated from Maxwell, 2019. Studies compare data from within burned forest (BF) unburned forest (UF), clearcut (CC) and open/SNOTEL areas.

More recently, the miniaturization of LiDAR instruments has enabled them to be installed on uncrewed aerial systems (UAS) which has several advantages over aerial and satellite LiDAR platforms. UAS platforms can be deployed on demand, are relatively inexpensive, and can produce higher resolution data products. They are, however, limited in their coverage and require on the ground presence. Only a few UAS LiDAR studies for forest snow mapping have been published (Dharmadasa et al., 2023; Harder et al., 2020; Jacobs et al., 2021; Koutantou et al., 2022). While airborne LiDAR derived snow depths have been used to study wildfire (Harpold et al., 2014), to our knowledge, no study has employed UAS LiDAR to measure snow depth distributions in a post-wildfire landscape.

Here we investigate the effects of a large wildfire on snowpack dynamics at a field site in the seasonal snow zone of the Western Cascades. To do this, we deploy a UAS LiDAR to map snow depth spatial distributions in an adjacent burned and unburned forest before, during, and after peak SWE during the 2022-2023 water year. This triplet of surveys enables investigation into the effects of wildfire on both snow accumulation and ablation processes. Since our study site is situated along a ridgeline, we extend previous wildfire-snow studies by sampling snow depths on both north- and south-facing slopes. We also extend previous wildfire-snow studies by sampling snow depths on steep slopes ranging from 16-33°. By doing so, our findings provide comprehensive insight into the response of snowpacks to wildfire, including their relationship with topographic controls.

2 STUDY AREA

Our field site is located in the western Oregon Cascades within a headwater catchment of the North Santiam River (Fig. 1). This site lies within the seasonal snow zone along a ridge line at approximately 44.8° latitude and 1300-1500 m above sea level (i.e. 250-450 m lower than the Gleason et al., 2013 field site). The site includes both north- and south-facing sides of the ridge top. Due to the circular nature of aspect, we report aspect values in "northness" values between +1 (due north) and -1 (due south), equal to the cosine of aspect in radians. The south-facing area has a slope of 21° ± 3° (mean ± std. dev.) and an aspect of -0.57 ± 0.09 (mean ± std. dev.). The north-facing area has a slope of 32° ± 5° (mean ± std. dev.) and an aspect of 0.72 ± 0.12 (mean ± std. dev.). Tree species at this site include North Pacific Dry-Mesic Silver Fir (*Abies alba*), Western Hemlock (*Tsuga heterophylla*), and Douglas-fir (Pseudotsuga menziesii). Timber resources in this basin have been selectively harvested, leaving behind a patchwork forest of different canopy conditions, from relatively open areas to full canopy (Fig. 1).

In 2020, our field site was impacted by the Lionshead Wildfire which burned over 826 km^2 of the Willamette National Forest and land belonging to the Confederated Tribes of Warm Springs Reservation near Mt. Jefferson (USFS, 2020). This wildfire began Aug 16, 2020, in Lionshead Canyon approximately 14 miles west of the Warm Springs community. On Sept 7, 2020, anomalously dry conditions coupled with strong east winds quickly grew the Lionshead Wildfire, which spread onto the Willamette, Deschutes and Mt. Hood National Forests (Reilly et al., 2022). Following the Lionshead fire, the Monitoring Trends in Burn Severity (MTBS) interagency program classified our field site area as 13 % low, 16 % moderate, and 71 % high burn severity (MTBS, 2022) (Fig. 1).

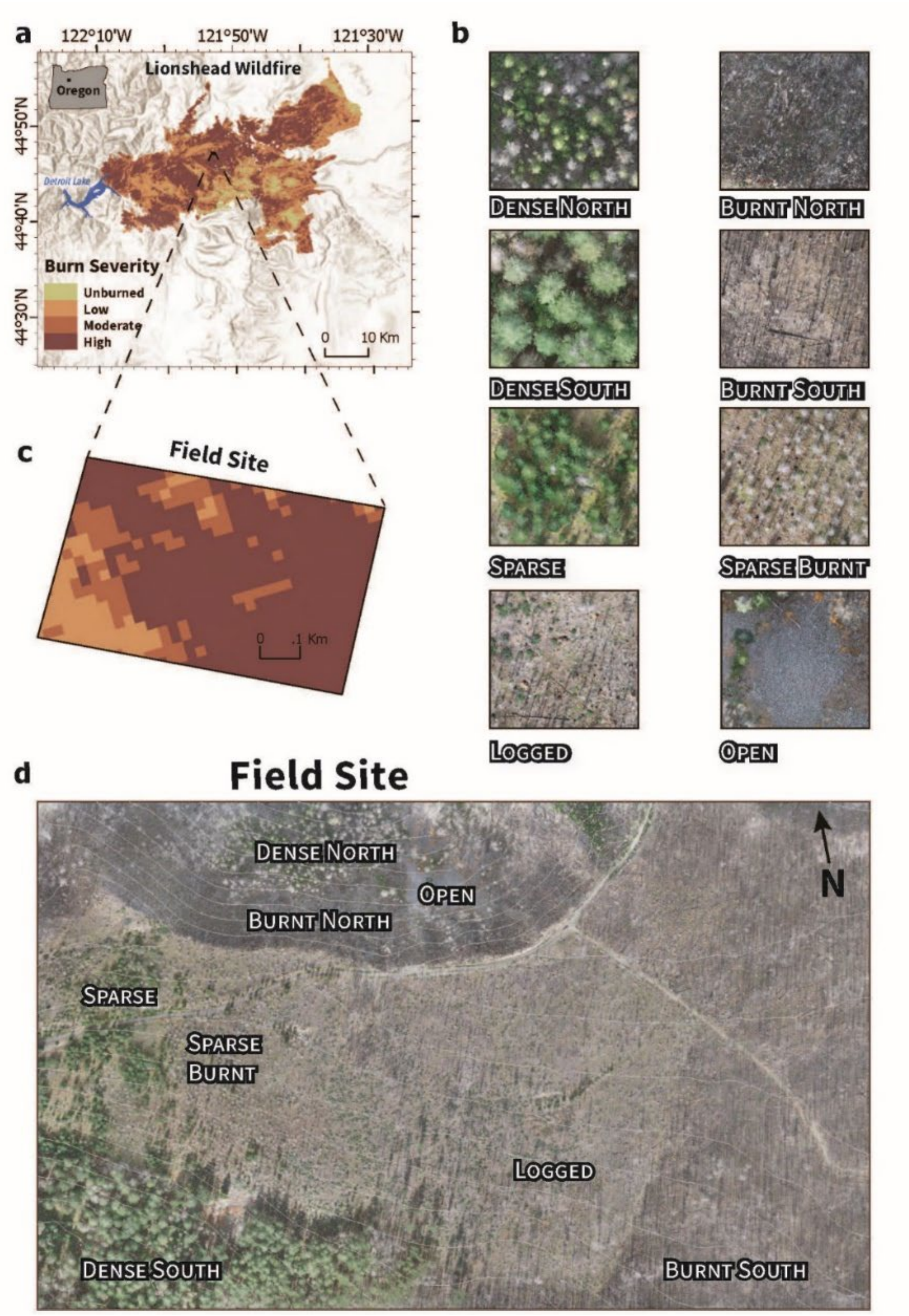

Figure 1. a) Lionshead Wildfire Perimeter displayed with MTBS burn severity data. b) Detail of areas within classes used in snow depth analysis. c) MTBS burn severity data within the field site. d) Snow-free orthomosaic of field site showing the approximate location of classes shown in b).

3 METHODS

3.1 DATA COLLECTION

We collected LiDAR data using a DJI L1 payload mounted on a DJI Matrice 300 quadcopter. The L1 contains a Livox Avia sensor modified for use with DJI drones. It operates in the near-infrared range (905 nm), has a detection range of 450 m, a field of view of 70.4° × 4.5° (horizontal x vertical) in repetitive scanning mode, and a point rate of up to 480,000 pts/s. The nominal accuracy of the L1 sensor is 10 cm (horizontal) and 5 cm (vertical). The L1 includes an integrated Inertial Measurement Unit (IMU) system with an update frequency of 200 Hz and a post-processed accuracy of 0.025°(roll/pitch) and 0.15°(yaw). The L1 also includes a 20MP RGB mapping camera with a 1-inch sensor which is useful for generating orthomosaics of the study site.

We acquired snow-covered LiDAR data over a 0.5 km^2 area on three days during the 2023 water year (Mar 21, Apr 14, May 01), with snow-free data collected on July 21. We developed flight paths in DJI Pilot 2 software and collected both LiDAR and RGB data on all surveys. There are several parameters that can be customized on DJI Pilot 2. We opted for a triple return mode with the highest available sampling rate (160 Hz) to maximize the number of returns from beneath the canopy. We chose a 6 m/s flight speed and 50% side overlap to optimize return densities while providing enough coverage to complete the survey using our six available batteries. We chose repetitive scanning mode as it provides a narrower field of view and higher accuracies than the non-repetitive scanning mode. As no digital elevation model was available at the beginning of the project, Mar 21 and Apr 14 flights were flown at a consistent altitude of 100 m and 60 m *above the take-off point*, respectively. These settings resulted in an average return density of 166 pts/m^2 over an area of 0.96 km^2 for the March survey, an average return density of 196 pts/ m^2 over 0.96 km^2 for the April survey. In contrast, by utilizing Terrain Following mode the UAS maintained a consistent 100 m and 60 m height *above the surface*, for the May 1 and Jul 21 surveys, respectively. These settings resulted in an average return density of 396 pts/m^2 over 0.87 km^2 for the May survey, and an average return density of 745 pts/m^2 over 0.81 km^2 area for the July survey.

To accurately geolocate the LiDAR data, we installed three benchmarks to enable Real Time Kinematic (RTK) and Post Processed Kinematic (PPK) GNSS techniques. The benchmarks consisted of a metal T-post driven into the ground surface, anchored by guy lines attached to rebar (Fig. 2). The top of each benchmark consisted of a short section of survey pole affixed to the anchored T-post with the male end facing upwards. A small divot was drilled into the center of the male end, allowing the pointed end of the dRTK base station pole to sit securely on top of the monument. We performed Precise Point

Positioning (PPP) GNSS surveys of between 4 and 24 hours to determine the precise positions of these benchmarks. During each UAS survey, our DJI dRTK base station was placed on one of these benchmarks to enable RTK positioning. We processed GNSS data from PPP surveys using the online Canadian Spatial Reference System (CSRS) PPP utility (https://webapp.csrs-scrs.nrcan-rncan.gc.ca/geod/tools-outils/ppp.php). Height differences between the bottom of the base station GNSS receiver and the pointed dRTK base station were manually measured and accounted for during post-processing.

We collected auxiliary in-situ snow depth data using an avalanche probe and a pair of Emlid RS2+ GNSS receivers to validate our UAS-derived snow depths. During in-situ snow depth data collection, we threaded a single GNSS receiver on to one of our monuments to serve as a base station while the second GNSS receiver served as a rover to collect snow depth measurement position data. Snow depth measurements were acquired within three hours after UAS missions so as not to disturb the snow surface. The positions of snow depth measurements were averaged over 1-minute occupation times. We processed GNSS data from in-situ snow depth surveys using Emlid Studio software. We collected a total of 32 snow depth measurements during the 2022/2023 season. We compared in-situ and UAS-derived snow depths using the XY data from our GNSS survey points to extract snow depth data from pixels in our dDTM.

3.2 DATA PROCESSING

3.2.1 SNOW DEPTHS

We produced snow depth distribution and forest canopy structure products from the LiDAR point cloud data after cropping it to our study area polygon (Fig. 1). Digital Terrain Models (DTMs), derived from only ground-classified points, are a type of Digital Elevation Model (DEM). In contrast, Digital Surface Models (DSMs) are DEMs created from all points, including canopy and non-ground points. For initial processing, we used DJI TERRA to classify ground points. Through trial and error, we found that the following settings yielded the highest fidelity ground classification based on visual inspection: a 300 m point cloud effective distance, point cloud accuracy optimization on, steep group type, building max diagonal of 10, 10 iterations, and an iteration distance of 0.7.

Subsequently, we imported the data into an R environment for checking, cleaning, thinning, and rasterization. To produce DTMs for both snow-covered and snow-free conditions, we employed a triangular irregular network (TIN) algorithm with Delaunay triangulation to interpolate spatially between points. By differencing our 10 cm resolution snow-covered (Mar 21, Apr 14, May 01) and snow-free DTMs (Jul 21), we created snow depth maps.

Figure 2.GNSS monument composed of a T-post and guy lines anchored to rebar. b) Emlid RS2+ GNSS receiver and several sections of survey pole affixed to monument. c) DJI dRTK-2 GNSS station over GNSS monument. d) UAV landing after a completed flight mission.

3.2.2 OTHER PRODUCTS

We produced a canopy height model (CHM) from the Jul 21 snow-free survey using a DSM TIN algorithm with Delaunay triangulation. From the CHM, we generated a binary canopy presence map using a height threshold of over 2 m, following the methods of Broxton et al. (2015) and Mazzotti et al. (2019). Using the RGB photos collected by the UAS, we also generated orthomosaics of both snow-covered and snow-free conditions in Agisoft Metashape Pro using the RGB photos collected by the UAS.

3.3 ANALYSIS

3.3.1 DATA AGGREGATION

We prepared our data for analysis by aggregating our 10 cm dDTMs and CHM onto a hexagonal grid with a diameter of 15 m. We used a hexagonal grid because hexagons have a higher degree of symmetry compared to square grids, with the angles between adjacent hexagons all being 120° and equidistant. We opted for 15 m diameter hexagons because this size provided a good balance between reducing noise and accurately representing variability across the landscape. The 15 m hexagons contain enough 10 cm pixels to provide robust mean values of snow depth and canopy data but are small enough to accurately represent the spatial heterogeneity of our field site. We extracted slope, aspect, and elevation data from the snow-free DTM and calculated the mean values of pixels falling within each hexagon. Similarly, we calculated mean values of canopy cover (%) for each hexagon area.

3.3.2 CATEGORY SELECTION

Our field site contains not only a variety of burn severity and aspect, but also varying forest canopy cover (Fig. 1, Fig. 4). To facilitate the comparison of snow depths in distinctly different areas of our field site, and to assess the impacts of severe wildfire on snow depth, we divided our field site into categories based on a snow-free orthomosaic (Fig.1), pre- and post-fire reflectance data from Sentinel-2 (Fig. 3), and the canopy height model (Fig. 4). In consideration of these goals, we classified our field site by manually selecting grid cells and placing them into the following categories: burned forest (BF), dense forest (DF), burned sparse forest (BSF), sparse forest (SF), logged (L) and open (O).

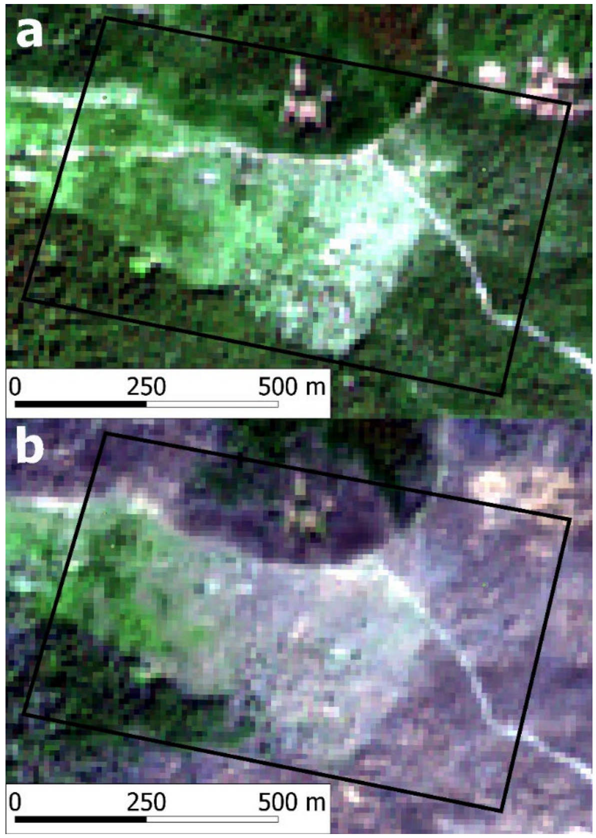

Figure 3. (a) Field site data extent (black polygon) over Sentinel-2 pre-fire August 10, 2020, data. (b) Field site data extent (black polygon) over Sentinel-2 post-fire August 10, 2022, data.

We decided on these categories because our field site not only contains low, moderate, and high severity burn (Fig. 1), but areas of distinctly different forest canopy resulting from historic logging activities (Fig. 4). Since aspect is a major control on snow depth at our site (Fig. 5), we differentiate between North and South aspect by appending a 'n' or 's' to the end of our category acronyms. For example, BFn refers to the burnt forest on the north facing slope whereas BFs refers to the burnt forest on the south facing slope. After separation into North and South groups, snow depths exhibited insignificant correlations with aspect (Tables 4, 5).

The characteristics of our categories can be found in Tables 2 and 3 but we also describe them here, starting with the forest categories on the south aspect. The difference between the dense forest (DFs) and sparse forest (SFs) are primarily related tree height and crown size. The DFs contains tall trees with large crown sizes while the SFs contains relatively short trees with smaller crown sizes. Canopy cover averages 72 % in DFs whereas it only averages 35 % in SFs. SFs represents an area of homogeneous age trees which grew following a disturbance (clearcut). The Lionshead wildfire burned this area in a mosaic pattern, severely burning some tree crowns and leaving some relatively intact (Fig. 1). Based on the orthomosaic and canopy height model, we selected grid cells containing severely burnt tree crowns in this area and placed them into the burned sparse forest south (BSFs) category. BSFs averages 10 % canopy cover and 82 % high severity burn according to MTBS, whereas SFs averages 35 % canopy cover and is mostly moderate and low severity burn (Table 3). Burnt forest south (BFs) represents an area not targeted by timber harvest that was severely burned by the Lionshead wildfire. Sentinel-2 images from before the wildfire on Sep 2020 indicate that this category has similar NDVI values to DFs on Aug 2020 (Fig. 3). Most of DFs (75 %) is low severity burn whereas the vast majority of BFs (98 %) is high severity burn (Table 3). A large area of this aspect was the target of a selective timber harvest and has been named logged (Ls). While much of Ls is severely burned second growth forest, large trees with comparable heights and crown sizes to those found in DFs remain standing (Fig. 1, Fig. 4). Canopy cover averages only 7 % in Ls.

On the north aspect, we have created three different categories: dense forest north (DFn), burnt forest north (BFn) and open north (On). Like DFs, DFn contains many tall trees with large canopy size, however DFn was more affected by the wildfire, with most of the area classified as moderate severity (48 %) and high severity (38 %) burn. The adjacent BFn category has an average burn severity of 91 %, contains comparatively short trees with smaller crown sizes and may also have been the target of clearcut logging activity. Canopy cover on the north aspect categories averages 40 % in the DFn, 12% in the BFn. The north aspect also contains an open talus slope (On) with minimal (7 %) canopy coverage (Fig. 1).

The pre-fire satellite images and the orthomoasic we produced from UAS imagery provide justification for our comparisons between the BF and BSF categories severely impacted by the Lionshead wildfire and the DF and SF categories which were less severely impacted (Fig. 1, Fig. 3).

Once we categorized our field site, we noticed several areas that were deemed unrepresentative of the broader study region. For example, two forest roads ran through our field site, creating an unnatural break in slope that could potentially trap windblown snow. Snow surfaces on these roads were disturbed by tracks and skis to access the field site. We therefore excluded all grid cells that contained road surfaces from the analysis (white grid cells, Fig 6). Some errors existed in the snow depth data due to points associated with low lying vegetation being misclassified as the ground surface, which were also excluded from the analysis (white grid cells, Fig 6). Finally, the mean elevation of some categories was higher than others due to an elevation gradient across our field site.

North	Canopy Height (m) ± SD	Canopy Presence (%) ± SD	Slope (deg.) ± SD	Aspect (northness) ± SD	Elevation (m) ± SD	Low Severity (%)	Mod. Severity (%)	High Severity (%)
Dense Forest	4.8 ± 2.5	40 ± 16	33 ± 4	0.73 ± 0.14	1400 ± 22	14	48	38
Dense Burnt	0.9 ± 0.5	12 ± 7	33 ± 3	0.71 ± 0.14	1430 ± 15	1	8	91
Open	0.9 ±0 .9	7 ± 7	31 ± 4	0.76 ± 0.12	1406 ± 19	26	48	26

Table 2. North aspect category attribute data.

South	Canopy Height (m) ± SD	Canopy Presence (%) ± SD	Slope (deg.) ± SD	Aspect (northness) ± SD	Elevation (m) ± SD	Low Severity (%)	Mod. Severity (%)	High Severity (%)
Dense Forest	19 ± 9.0	72 ± 20	22 ± 5	-0.50 ± 0.21	1357 ± 23	75	21	4
Dense Burnt	2.3 ± 1.9	17 ± 11	16 ± 2	-0.48 ± 0.13	1428 ± 18	0	2	98
Sparse Forest	2.9 ± 2.0	35 ± 20	29 ± 3	-0.67 ± 0.11	1406 ± 20	31	55	14
Sparse Burnt	0.7 ± 0.6	10 ± 7	24 ± 4	-0.61 ± 0.10	1424 ± 17	4	14	82
Logged	1.0 ± 1.3	7 ± 6	19 ± 3	-0.63 ± 0.11	1426 ± 17	0	3	97

Table 3. South aspect category attribute data.

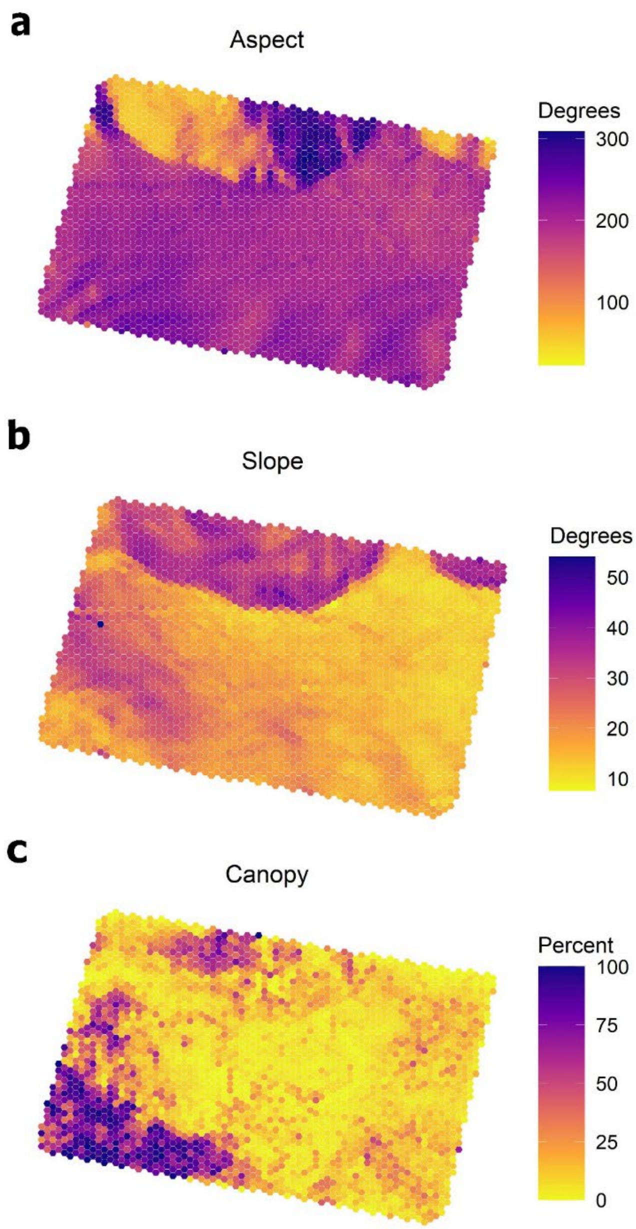

Figure 4. a) Mean aspect derived from the snow-off DTM averaged over each grid cell. b) Mean slope derived from the snow-off DTM averaged over each 15 m diameter hexagon area c) Canopy cover over 2 m derived from snow-free Jul 21 data.

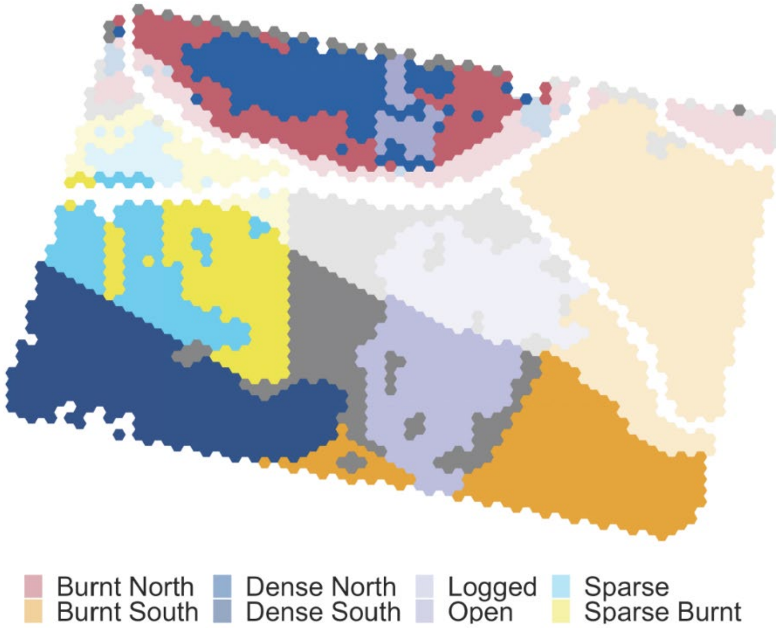

Figure 5. Manually selected grid cells colored by the spatial categories we used in our analysis. Opaque grid cells below our 1450m threshold were excluded from our analysis. White colored grid cells represent road surfaces, ridge tops or errors also excluded from our analysis. Grid cells without a category are grey in color.

Since elevation is known to have an important impact on snow accumulation and ablation, we therefore excluded grid cells from the upper elevations of our field site (>1450 m) from the analysis to ensure that our categories were comparable. This also served to reduce the number of hexagons within the BFs category so that the number of hexagons in the BFs, DFs and Ls categories were more similar (Fig. 6).

3.3.3 STATISTICAL ANALYSIS

We performed statistical analysis in a three phased approach. We first performed standard Pearson's r correlations on our grid cell data (divided into north and south aspects) to identify the primary controls on snow depth. Because we suspected multicollinearity between our independent predictor variables, we also calculated Pearson's r correlations between the predictor variables (slope, aspect, elevation, and canopy cover). Second, we performed a semi partial correlation analysis to independently evaluate the role of our two strongest predictor variables (elevation and canopy cover) on our snow depth patterns. Third, since initial conditions for ANOVA were not met, we used a Kruskal-Wallis Test to determine whether there were significant differences in snow depths between our categories (Fig. 5). To evaluate the impact of wildfire on snowpack, we perform paired tests between our categories.

4 RESULTS

4.1 ACCURACY ASSESSMENT

Our in-situ measurements collected on May 1 compared well against our dDTM snow depth data. We compared pixel values from our full 10 cm resolution dDTM against our in-situ measurements. The simple mean difference between our dDTM snow depths and our manually probed snow depths was + 8 cm (Fig. 6). This error includes both that associated with GNSS system accuracy, LiDAR ranging accuracy, and that associated with probing snow depths (the probe either not passing all the way through the snowpack or penetrating the ground surface). Probed snow depths were, on average, slightly deeper than dDTM snow depths for the May 1 survey. We hypothesize that this bias could be attributed to the avalanche probe penetrating a few centimeters into the ground surface, leading to probe depths that are biased high.

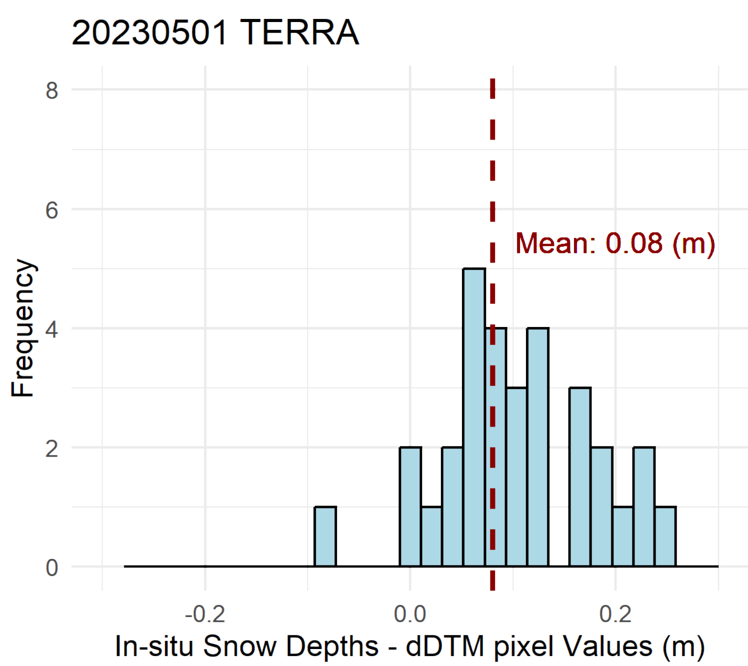

Figure 6. Manual snow depth measurements from May 1 subtracted from our May 1 dDTM generated from ground points classified in DJI TERRA software.

To place our three UAS survey dates in the context of peak SWE, we compared our survey dates with continuous SWE time series data from nearby Little Meadows SNOTEL station. Little Meadows SNOTEL sits at an elevation of 1225 m in Linn County, Oregon ~33 km from the field site. Survey dates are plotted as vertical dashed lines over Little Meadows SWE time series data in Fig. 8.

Our UAS LiDAR survey on Mar 21 was collected prior to peak SWE during the accumulation season (Fig. 8). Our Mar 21 snow depth data shows large spatial variation across the field site, with increased snow depths on north aspects (1.69 ± 0.30 m [mean ± std. dev.]) relative to south aspects (0.94 ± 0.19 m; Fig 4a). Initial qualatative visual comparisons between snow depths and canopy cover seem to indicate that open or burned areas of our field site are associated with higher snow depths while forested areas are associated with lower snow depths (Fig. 4, Fig. 7). Our survey on Apr 14 was collected near Peak SWE and the end of the accumulation season (Fig. 8). On Apr 14, we observe widespread increases in snow depths across the study area relative to Mar 21. Snow depths averaged 2.20 ± 0.30 m on the north aspect and 1.21 ± 0.22 m on the south aspect (Fig. 4). We also observe similar spatial patterns in snow depth which, again, appear to be associated with forest canopy effects. Finally, our survey from May 1 was collected after Peak SWE during the ablation season (Fig. 8). We observe widepread decreases in snow depths across the field site, with some areas completely devoid of snow cover. Snow depths are lower on May 1 than Apr 14 and also lower than Mar 21, averaging 1.35 ± 0.34 m on the north aspect and 0.52 ± 0.24 m on the south aspect. On May 1, ~8 % of our study site had mean snow depth < 10 cm. We explore the importance of our predictor variables in a more quantitative manner in the next sections.

4.2 CORRELATION MATRICIES

We performed standard Pearson's r correlations between Mar 21, Apr 14 and May 1 snow depth, slope, aspect, canopy cover and elevation grid cell data divided into north and south facing aspect groups to provide a more quantitative assessment of controls on snow depths across our field site. Pearson’s r correlation r values are summarized in Tables 4 and 5 below.

4.3 SNOW DEPTHS OVER TIME

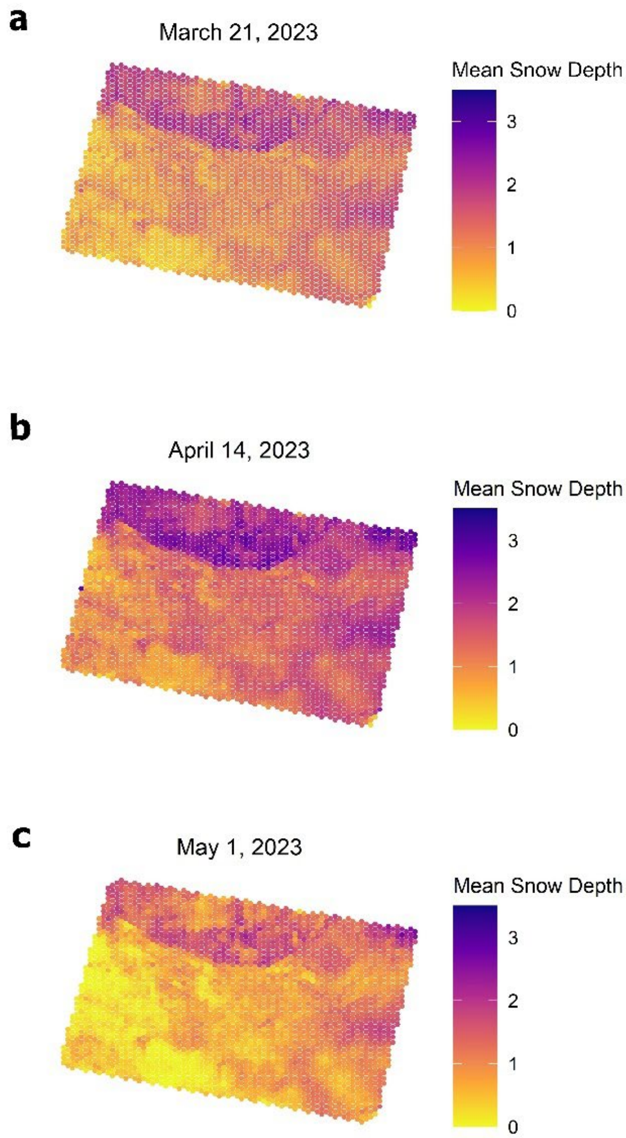

Figure 7. Aggregated dDTM snow depth data from Mar 21, Apr 14, May 1 UAS cropped to our field site polygon.

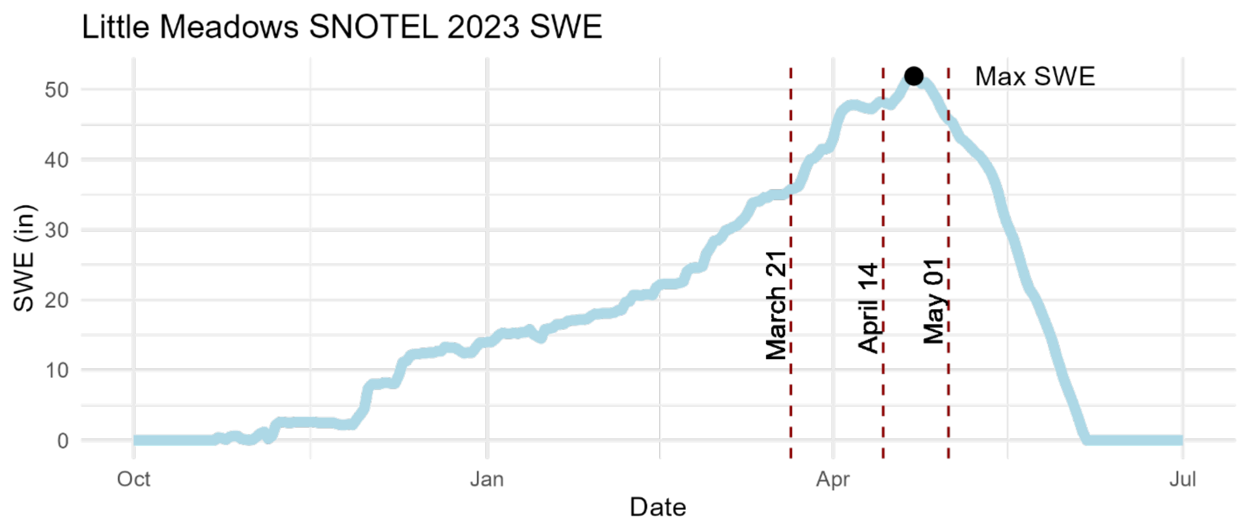

Figure 8. Little meadows SNOTEL 2023 Water Year SWE time series data (light blue line) showing the timing of UAS survey dates (red dashed lines). Little Meadows sits at an elevation of 1225 m in Linn County, Oregon.

North aspect	SD March 21	SD April 14	SD May 01	Slope	Aspect	Elev-ation	CC
SD March 21	1.00	0.99	0.95	-0.19	-0.04	0.57	-0.80
SD April 14	0.99	1.00	0.95	-0.10	0.07	0.56	-0.78
SD May 01	0.95	0.95	1.000	-0.26	0.00	0.50	-0.76
Slope	-0.19	-0.10	-0.26	1.00	0.49	0.09	0.15
Aspect	-0.04	0.07	0.00	0.49	1.00	0.02	0.19
Elevation	0.57	0.56	0.50	0.09	0.02	1.00	-0.45
CC	-0.80	-0.78	-0.76	0.15	0.19	-0.45	1.00

Table 4. Pearson's r correlation r values for the north aspect grid cell data. SD is short for snow depth and CC for canopy cover.

We find that, for the north aspect, canopy cover exhibits the strongest correlation with snow depth across all three survey dates (-0.80, -0.78, -0.76). Snow depths exhibit a moderate correlation with elevation (+0.57, +0.56, +0.50). However, elevation also has a moderate correlation with canopy cover (-0.45) suggesting that elevation and canopy cover are related, and therefore multicollinearity is present in our predictor variables. This is not surprising given the distribution of canopy cover on the north aspect (Fig. 1, Fig. 4). Slope showed a weak relationship with snow depth (-0.19, -0.10, -0.26).

South Aspect	SD March 21	SD April 14	SD May 01	Slope	Aspect	Elevation	CC
SD March 21	1.000	0.98	0.92	-0.42	0.05	0.58	-0.75
SD April 14	0.98	1.00	0.95	-0.48	0.14	0.51	-0.69
SD May 01	0.92	0.95	1.00	-0.63	0.25	0.49	-0.62
Slope	-0.42	-0.46	-0.62	1.00	-0.46	-0.26	0.22
Aspect	0.05	0.14	0.25	-0.46	1.00	-0.19	0.15
Elevation	0.58	0.51	0.49	-0.26	-0.19	1.00	-0.75
CC	-0.75	-0.69	-0.62	0.22	0.15	-0.75	1.00

Table 5. Pearson's r correlation r values for the north aspect grid cell data. SD is short for snow depth and CC for canopy cover.

Similarly, on the south aspect, canopy cover exhibits the strongest correlation with snow depth for each survey (-0.75, -0.69, -0.62). Elevation is moderate correlation (+0.58, +0.51, +0.49) with snow depth. However, elevation shows a strong correlation with percent canopy (-0.75), again, an unsurprising result given how canopy cover is distributed (Fig. 1, Fig. 4). Interestingly, the strength of the correlation between snow depth and slope increases over the three survey dates (-0.42, -0.46, -0.62) and we hypothesize that reflects steeper slopes receiving more direct solar radiation due to higher incidence angles, and importance of solar radiation on south aspects during the melt season. Given that the mean slope of the categories we compare only varied by a maximum of ± 6° (Tables 3 and 4) we did not account for differences in slope between our categories.

The correlations between elevation and snow depth were concerning given our desire to assess the influence of wildfire and canopy cover on snow depth and directly compare category pairs. For example, our DFs category had a mean elevation of 1357 m ± 23 m (mean ± std. dev.), which is lower than the categories we were aiming to compare it against; BFs (1428 m ± 18 m) and Ls (1426 ± 17). To address this, we examined grid cell data from all three of these categories, plotting snow depth against elevation and snow depth against percent canopy cover. Both DFs and Ls showed no correlation, but we did observe a significant positive correlation between snow depth and elevation in the BFs and a significant negative relationship between elevation and canopy cover. We therefore suspected that collinearity between canopy cover and elevation was responsible for the observed relationship between snow depth and elevation. To evaluate this hypothesis, we performed a semi partial correlation to our data, split into N and S aspects. The semi partial correlation allowed us to isolate the unique impact of one predictor variable (i.e. canopy cover) on the dependent variable (i.e. snow depth) while controlling for another independent variable (i.e. elevation) (Kim, 2015).

North Semi-partial correlation	Controlling for: Canopy Cover	Controlling for: Elevation
March 21	0.230***	-0.589***
April 14	0.231***	-0.575***
May 1	0.180**	-0.581***

Table 6. Semi partial correlation r values for the north aspect grid cells. Asterisks indicate significance levels.

South Semi partial correlation	Controlling for: Canopy Cover	Controlling for: Elevation
March 21	0.028	-0.474***
April 14	-0.016	-0.469***
May 1	0.031	-0.386***

Table 7. Semi partial correlation r values for the south aspect grid cells. Asterisks indicate significance levels.

On the south aspect, after controlling for canopy cover, we find that there is no statistically significant relationship between elevation and snow depth over all three survey dates (0.03, -0.02, 0.03) (Table 7). Conversely, after controlling for elevation, canopy cover still has a significant moderate correlation with snow depth (-0.47, -0.47, -0.39) (Table 7). We therefore conclude that elevation has negligible influence on snow depths on the south aspect of our field site below 1450 m and proceed with direct snow depth comparisons between BFs, DFs and Ls. On the north aspect, after controlling for canopy cover, elevation did show a significant weak linear relationship with snow depths (+0.23, +0.23, +0.18). From this analysis we conclude that elevation has an influence on snow depth on the north aspect of our field site even after controlling for the effects of canopy cover. Given that there are differences in mean elevation between BFn and DFn of 30 m (Table 2), and a 24 m difference between DFn and On, we cannot exclude the impact of elevation on our direct snow depth comparisons between categories on the north aspect (Table 8; Fig. 9).

4.4 SNOW DEPTHS BY CATEGORY

We find that snow depths are significantly greater in the burned forest categories relative to their corresponding forest categories for both aspects (Tables 8 and 9; Figs. 9 and 10). Over the three surveys for our South aspect comparisons, we found greater mean snow depth in BFn (1.86 ± 0.14 m, 2.39 ± 0.16 m, 1.53 ± 0.18 m [mean ± std. dev.]) than in the DFn (1.47 ± 0.22 m, 1.96 ± 0.23 m, 1.11 ± 0.27 m). Similarly, we found greater mean snow depth in BFs (1.15 ± 0.24 m, 1.45 ± 0.28 m, 0.79 ± 0.29 m) than in DFs (0.64 ± 0.18 m, 0.92 ± 0.20 m, 0.26 ± 0.19 m) and greater mean snow depth in SBFs

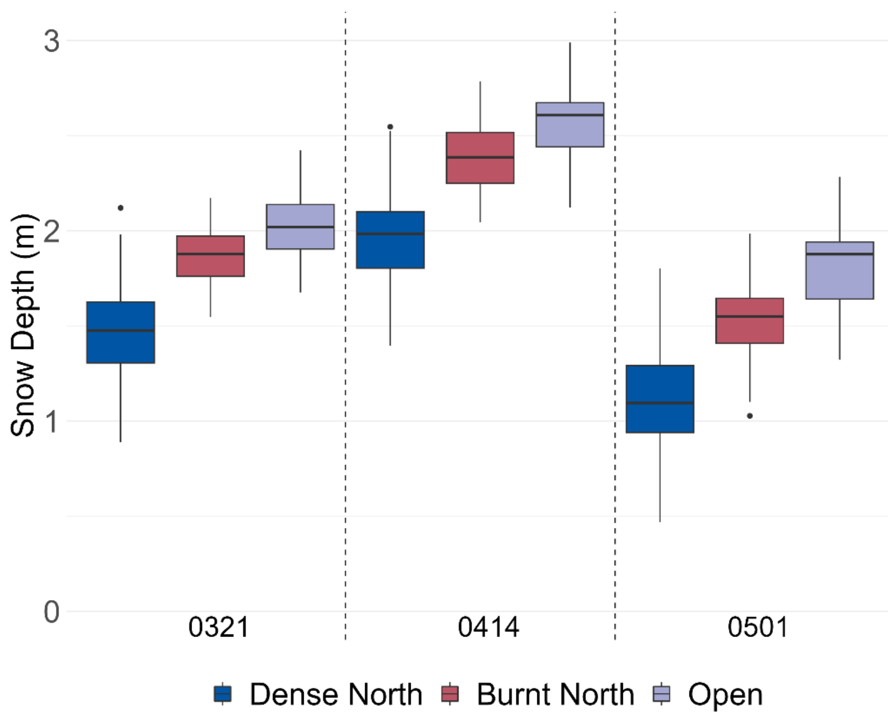

Figure 9. North aspect Dense Forest, Burnt Forest, and Open category grid cell snow depth data boxplots.

North	Snow Depth 0321 (m) ± SD	Snow Depth 0414 (m) ± SD	Snow Depth Difference 0321 to 0414 (m) ± SD	Snow Depth 0501 (m) ± SD	Snow Depth Difference 0414 to 0501 (m) ± SD
Dense North	1.47 ± 0.22	1.96 ± 0.23	0.49 ± 0.05 (2.0cm/day)	1.11 ± 0.27	-0.86 ± 0.10 (-5.1 cm/day)
Burnt North	1.86 ± 0.14	2.39 ± 0.16	0.52 ± 0.05 (2.2cm/day)	1.52 ± 0.18	-0.86 ± 0.10 (-5.1 cm/day)
Open	2.01 ± 0.15	2.56 ± 0.18	0.55 ± 0.05 (2.3cm/day)	1.82 ± 0.21	-0.74 ± 0.06 (-4.4 cm/day)

Table 8. North aspect category mean snow depth data and snow depth difference between survey dates.

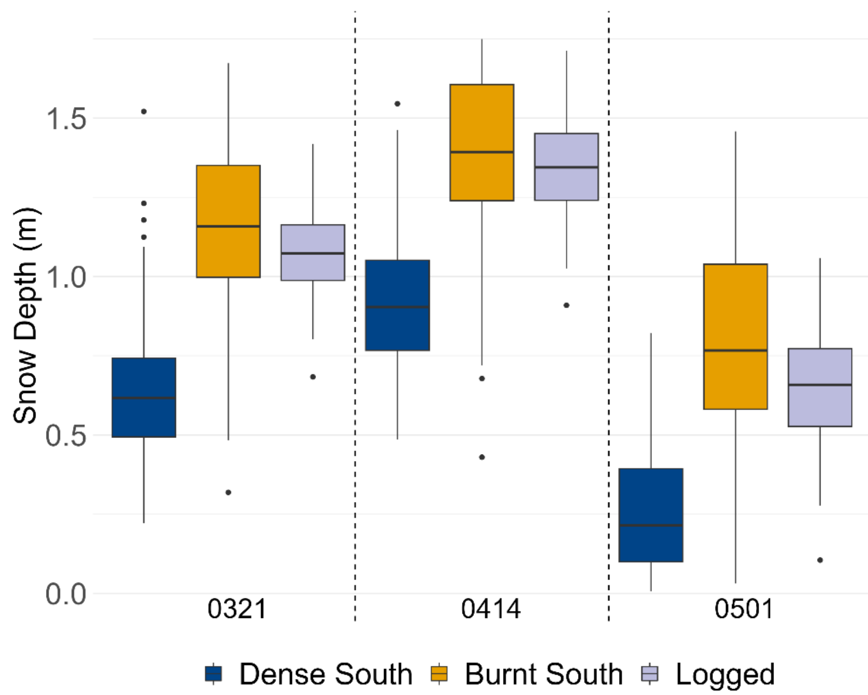

Figure 10. South aspect Dense Forest, Burnt Forest, and Logged category grid cell snow depth data boxplots

South	Snow Depth 0321 (m) ± SD	Snow Depth 0414 (m) ± SD	Snow Depth Difference 0321 to 0414 (m) ± SD	Snow Depth 0501 (m) ± SD	Snow Depth Difference 0414 to 0501 (m) ± SD
Dense South	0.64 ± 0.18	0.92 ± 0.20	0.29 ± 0.08 (1.2cm/day)	0.26 ± 0.19	-0.66 ± 0.11 (-3.9 cm/day)
Burnt South	1.15 ± 0.24	1.45 ± 0.28	0.30 ± 0.05 (1.3cm/day)	0.79 ± 0.29	-0.66 ± 0.07 (-3.9 cm/day)
Sparse	0.77 ± 0.20	1.00 ± 0.25	0.22 ± 0.07 (0.9cm/day)	0.24 ± 0.18	-0.76 ± 0.12 (-4.4 cm/day)
Sparse Burnt	1.00 ± 0.20	1.25 ± 0.24	0.26 ± 0.05 (1.1cm/day)	0.51 ± 0.26	-0.74 ± 0.09 (-4.4 cm/day)
Logged	1.07 ± 0.12	1.34 ± 0.15	0.27 ± 0.03 (1.1cm/day)	0.65 ± 0.17	-0.69 ± 0.06 (-4.1 cm/day)

Table 9. South aspect category mean snow depth data and snow depth difference between survey dates.

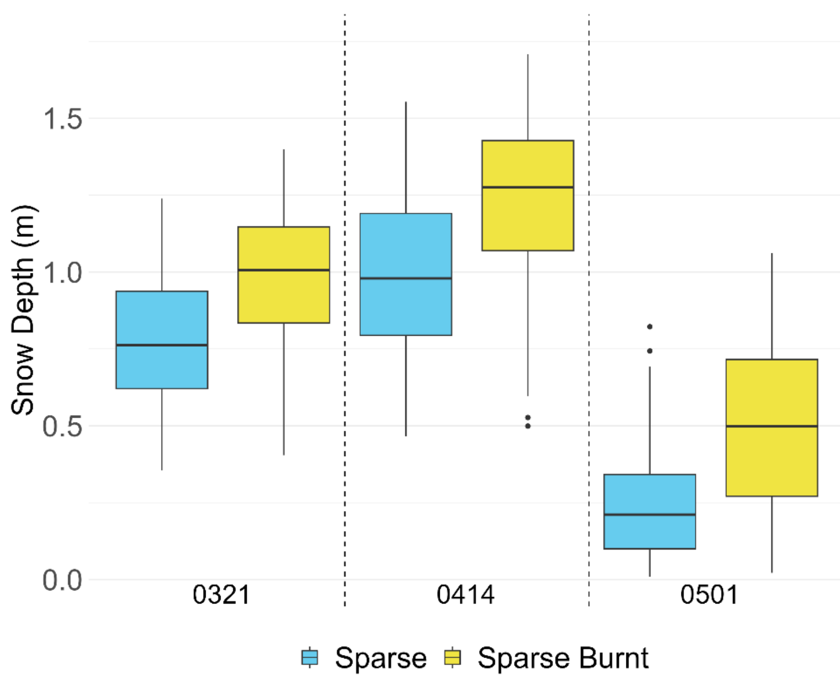

Figure 11. South aspect Sparse Forest and Sparse Burnt Forest category grid cell snow depth data boxplots

(0.99 ± 0.20 m, 1.25 ± 0.24 m, 0.50 ± 0.26 m) than in SFs (0.77 ± 0.20 m, 0.99 ± 0.25 m, 0.50 ± 0.26 m). A useful control is that the greatest snow depth was consistently found in On, (2.01 ± 0.15 m, 2.56 ± 0.18 m, 1.82 ± 0.21 m) which contains the smallest canopy cover out of all the categories (Tables 2 and 3). These findings thus suggest that the Lionshead Wildfire, by modifying canopy cover, significantly increased snow depths in areas of high burn severity throughout the study period by removing canopy cover.

The only category comparison that was not significant was BFs vs. Ls, which was not significant for any date (Table 8). BFn vs. Significance levels less than 0.01 but greater than 0.001 were observed between BFn and On on Mar 21 and Apr 14 (Table 8). We attribute the lack of significant differences between BFs vs. Ls and reduced significance between BFn vs. On is likely to their similar mean canopy cover (Tables 2, 3).

Category Comparisons	March 21	April 14	May 1
Burnt South vs. Dense South	< 0.001	< 0.001	< 0.001
Burnt South vs. Logged	Not significant	Not significant	Not Significant
Dense South vs. Logged	< 0.001	< 0.001	< 0.001
Sparse Burnt vs. Sparse	< 0.001	< 0.001	< 0.001
Burnt North vs. Dense North	< 0.001	< 0.001	< 0.001
Burnt North vs. Open	< 0.01	< 0.01	< 0.001
Dense North vs. Open	< 0.001	< 0.001	< 0.001

Table 10. Kruskal-Wallis test results for each category comparison.

4.5 SNOW DEPTH CHANGE

Our snow depth maps provide insight into the effects of wildfire on peak snow depths. But since we surveyed our field site multiple times, our measurements also allow us to investigate the effects of wildfire on accumulation and ablation processes.

4.5.1 BETWEEN MAR 21 AND APR 14

We do not find significant differences in rates of snow accumulation between DFn, BFn and On for this period. We find that snow depth increased in the DFn by 0.49 m ± 0.05 on average between Mar 21 and Apr 14 (2.0 cm/day) 0.52 ± 0.05 m (2.2 cm/day) in the BFn. Snow depths in the Open category increased by 0.55 ± 0.05 m (2.3 cm/day). Again, the slightly higher rates of snow accumulation in the burned and open areas may be the result of decreased canopy interception in areas with lower canopy coverage (Table 2). It is worth noting that all north aspect categories had a greater increase in snow depth compared to the south aspect categories. This signifies that although there was net snow accumulation during this period, melt and/or snow compaction also occurred on the south aspect.

On the south aspect, we find no significant differences in mean snow depth between BFs and DFs or between SBFs and SFs over the period from Mar 21 to Apr 14. Snow depths increased in the BFs by 0.30 ± 0.05 m (mean ± std. dev.) on average between Mar 21 and Apr 14 (1.3 cm/day) and increased by a similar rate in the corresponding DFs (0.29 ± 0.08 m or 1.2 cm/day). Similarly, snow depths increased by 0.26 ± 0.05 m (1.1 cm/day) in the BSFs and increased by a similar rate in the SFs by 0.22 ± 0.07 m (0.9 cm/day). While not statistically significant, the slightly higher rates of snow accumulation in the severely burned areas during this period may be the result of decreased interception in the areas with lower canopy cover (Table 3).

4.5.2 BETWEEN APR 14 AND MAY 1

Surprisingly, we find no significant differences in rates of snow ablation between our paired categories on the south-facing aspect. We find that snow depth decreased in the BFs by -0.66 ± 0.11 m between Apr 14 and May 01 (-3.9 cm/day), decreased by -0.66 ± 0.07 m in the DFs (-3.9 cm/day), and -0.69 ± 0.06 m in the Ls (-4.1 cm/day). Snow depth decreased in the BSFs by -0.74 ± 0.09 m (equivalent to -4.4 cm/day) and by -0.69 ± 0.06 m (-4.1 cm/day) in the SFs. The slightly higher rate of ablation in the SFs and BSF relative to the BF and DF categories could be due to the higher slope values in those areas causing a more direct solar incidence angle.

North aspect ablation rates are, in general, larger than south aspect decreases during our ablation period. Like the south aspect, we find no significant differences in rates of snow ablation between our paired categories. Snow depth decreased in the BFn and DFn by -0.86 ± 0.10 m on average between Apr 14 and May 1 (equivalent to -5.1 cm/day) and decreased by -0.74 ± 0.06 m (equivalent to -4.4 cm/day) in the On. The lower ablation rate in the On category relative to its nearby forest categories could be due to the lack of tree canopy structure in this area (and thus little to no vegetation driven longwave radiation).

5 DISCUSSION

5.1 SUMMARY OF OUR FINDINGS

By comparing snow depths in forested areas impacted both by wildfire and timber harvest, our findings provide insight into the impacts of wildfire on snow dynamics in a maritime climate. We find large spatial variations in snow depths across our field site that are best explained by aspect and canopy cover (Tables 4 and 5). Once we account for aspect (by dividing our data into separate categories), we find the lowest snow depths in areas with the highest canopy cover (e.g. DFs, DFn) and the highest snow depths in areas with the lowest canopy cover (e.g. On, Tables 8 and 9). The severely burned areas of our field site (BFs, SBFs, and BFn) have significantly higher snow depths than adjacent forested areas less impacted by the fire both before and following peak SWE. Although we found canopy cover to be the dominant control on snow depth variability within our field site, canopy cover and snow depth have the weakest correlation on May 1 (Tables 4 and 5). We interpret this decrease in correlation strength between to be a result of a shift from accumulation to ablation season and a shift away from canopy interception being the dominant control on snow depth.

Our snow depth data from Apr 14, when measured depths were greatest, agrees with the only other study of snow-wildfire dynamics in the PNW which found that peak SWE was enhanced by 11% in a burned forest relative to unburned forest (Gleason et al., 2013; Gleason and Nolin, 2016). This finding is consistent with most of the snow-wildfire studies summarized in Table 1 ((Burles, 2011; Harpold et al., 2014; McGrath et al., 2023; Skidmore, 1994; Winkler, 2011).

We find that accumulation rates were slightly (but insignificantly) elevated in severely burned forests relative to forests less impacted by the fire between Mar 21 and Apr 14. We attribute this finding to increased canopy interception efficiency in areas with denser canopy structure. Interestingly, we find that decreases in snow depths between Apr 14 and May 1 were similar between severely burned forests and adjacent lower severity burned forests. This finding is inconsistent with all of the snow-wildfire studies summarized in Table 1 (Burles, 2011; Harpold et al., 2014; Maxwell et al., 2019; McGrath et al., 2023; Skidmore, 1994; Smoot and Gleason, 2021; Winkler, 2011). However, this discrepancy may be explained by placing both our findings and the other studies into climatic context. Almost all the other studies of wildfire and snow interactions were carried out in the cold, continental climates of the mountain west where open areas are known to experience higher rates of mid-winter ablation and snow transport. For example, significantly more ablation (47% of winter precipitation) was observed prior to peak snowpack in a post-burn area relative to healthy forest in New Mexico (Harpold et al., 2014). In

Colorado, SWE gains in a burned area attributed to a loss of forest canopy interception were exceeded by losses attributed to mid-winter melt and increased sublimation (McGrath et al., 2023). It is therefore not surprising that ablation season melt rates are enhanced by wildfire in cold continental climates of the mountain west.

There are several reasons that may explain differences between our findings, and the findings in Gleason et al. (2013) and Gleason and Nolin (2016), which compared snowpack at the edge of the Shadow Lake wildfire burn scar in the Oregon Cascades at an elevation of 1750 m using paired meteorological stations and in-situ measurements in burned and unburned forests. This study found higher snow ablation rates in burned forests relative to unburned forests. During the ablation period, net shortwave radiation was over 200 % greater in the burned forest (Gleason et al., 2013). The removal of canopy cover by wildfire allowed increased transmission of shortwave radiation, and, coupled with enhanced absorption driven by the presence of black carbon and burned woody debris concentrations caused snow accelerated ablation rates.

We, however, find similar snow depth decreases in severely burned forests with and lower severity burn forests on both aspects between Apr 14-May 1, indicated that there was a balance between shortwave and longwave driven snow melt during this period. Furthermore, some unburned areas of the south aspect (especially in DFs and SFs) were snow-free by May 1, and therefore could not melt anymore, meaning that our ablation rates in these areas are conservative. Higher rates of melt in the relatively intact forests would imply that the longwave radiation emitted by trees was the dominant term in the surface energy balance even on steep south facing aspects in the ablation season. We observed greater snow depth decreases in the moderately burned DFn and severely burned BFn relative to the On talus slope, which provided a good control to assess how the presence of burned and trees impacted snow depth loss.

A four-year study in the Oregon Cascades examined snowpack in open and forest site pairs at three elevations: Low (1150 m), Mid (1325 m) and High (1465 m) using met stations, snow depth and SWE measurements found that the Pacific Northwest snowpack is sensitive to temperature and forest cover (Roth and Nolin, 2017). Interestingly, this work found that snowpacks were *deeper* and *lasted longer* in open sites at the Low and Mid elevations, but that the relatively colder high sites displayed the opposite relationship, with the forests site retaining snow longer. This finding was attributed to the high canopy interception efficiency of relatively warm forests and a shift from shortwave to longwave radiation as the dominating term in the energy balance (Lundquist et al., 2013; Roth and Nolin, 2017; Storck et al., 2002). Since the study by Gleason (2013) took place 250-450 m higher than our site and nearer to the peak of the

Cascade crest, we hypothesize that differences in climate between the two sites are substantial and may help explain the observed differences.

Previous research has found that regions with average December-January-February (DJF) temperatures greater than 1 C, forests with lower total canopy cover are likely to enhance snow retention by minimizing mid-winter and early spring melt (Lundquist et al., 2013). In maritime climates, such as the PNW, the effects of wildfire are likely to be more complex due to compensating factors. The differences in snow ablation rates between our study and Gleason et al. (2013) imply that the effects of wildfire on snowpack dynamics can be highly variable in maritime climates due to differences in microclimate even within a relatively short distance and range in elevation.

5.2 DOWNSTREAM IMPACTS

The amount and timing of surface water derived from snowmelt in the Roaring Creek basin determines availability of water resources used for drinking and irrigation. If, as we have found in this study, near peak SWE and mid ablation season snow depths are increased by the removal of tree canopy in severely burnt areas, severe wildfire could potentially increase late season snow derived water resources in some areas. As wildfire affects more and more land in the Pacific Northwest, and both total snowfall and the proportion of precipitation falling as snow decreases, understanding the how wildfire affects snow processes in this region is increasingly important to making appropriate water management decisions and ensuring the availability of water resources.

5.3 REFLECTION ON TECHNOLOGY

In this study, we used UAS LiDAR to retrieve accurate elevation models across a 0.5 km2 field site to investigate the impacts of wildfire on snowpacks. UAS LiDAR dramatically improves spatial coverage compared to traditional manual and meteorological in-situ measurements. Passive optical stereophotogrammetry sensors are unable to map snow depth mapping beneath dense forests. LiDAR, on the other hand, can collect ground surface data underneath canopy cover because of the ability of laser pulses to penetrate tree canopy structure. We believe that UAS LiDAR has much potential for increasing our understanding of snow processes, particularly small scale processes, in forested areas.

Multirotor UAS LiDAR has both advantages and disadvantages relative to airborne LiDAR platforms used to measure snow depth. Airborne LiDAR systems (ALS) is a valuable tool in snow depth mapping. However, ALS data products can have data gaps underneath tree canopies (Broxton et al., 2015; Mazzotti et al., 2019). Steep terrain can also be a challenge for ALS, leading to increased vertical inaccuracies especially in satellite and airborne systems with large laser footprints. As distance is increased between the sensor and the target, laser footprint size increases and point densities decrease (Figure 12). UAS LiDAR is an alternative to ALS that can be deployed on demand. With the ease of deployment comes the option to fly UAS LiDAR at various scanning angles (Koutantou et al., 2022) to maximize sub canopy ground returns, a substantial advantage over an acquisition at a single scan angle. Multi-rotor UAS have an advantage over fixed wing platforms in steep terrain due to their ability to hover. This ability translates into a setting called terrain following, in which the UAS maintains a constant altitude above a DEM loaded into the UAS controller, which allows for maximum sub canopy returns.

5.4 LIMITATIONS

Our field site was selected because it included both north and south facing aspects and large variations in canopy cover due to heterogeneous effects of wildfire. However, because we were comparing snow depths across space, there were small differences in slope, aspect, and elevation between our categories with the exception of the second growth forest categories. Small differences in slope, aspect, elevation remained that could have an impact on our results. Harpold et al. (2014) suggested that other variables (elevation, latitude, and slope) could be having a larger effect on ablation rates than burn condition alone at their field site in Utah. For a more direct comparison, a simpler site could be selected with identical slope, aspect, and elevation.

It should also be reiterated that this study is not a comparison between unburned and burned forests, as the entirety of our field site was within the burn perimeter and had burn severity ranging from low to high (Fig. 1). If this comparison is the goal, there are advantages to having paired sites a distance away from each other as in (Winkler, 2011) because it is possible that the impacts of the wildfire extend beyond the wildfire perimeter.

Our hypothesis that longwave radiation was the dominant term in the energy balance and caused the observed changes in snow depth, while consistent with previous research in unburned areas, is not based on in-situ data. Additional studies using data from automated meteorological stations of air temperature and radiative energy balance would help to shed light on these processes in a highly variable region sensitive to changes in temperature and forest cover.

5.5 RECOMMENDATION FOR FUTURE STUDIES

When studying snowpack processes in forested areas, the distance from the drone to the ground surface (DTM), and not the tree tops (DSM) should be kept constant during the survey. This means the DEM loaded into the UAS controller should be a DTM, and in areas with tall tree canopies, the terrain flight mission height should ideally be set to just a few meters above the height of the tallest tree.

Our flight setting included a 6 m/s flight speed and 50% side overlap to provided high return densities and enough coverage to complete the survey using our 6 available batteries. We recommend slower flight speeds (3m/s) and interlaced scan patterns (combining data from multiple surveys oriented at different scan angles, for example, facing the 4 cardinal directions) when collecting ground surface data in dense forest canopies (Koutantou et al., 2022).

6 CONCLUSION

We used a UAS LiDAR to investigate the extent to which wildfire impacts snowpack depths in a forested area with historic logging activity and varied burn severity covering both north and south aspects. We collected snow depth data over three surveys representing before, near and after peak SWE which allowed us to examine periods during both the snow accumulation and ablation season. After aggregating our data, we performed statistical tests on grid cell data to examine the correlations between snow depth, aspect, elevation, and canopy cover. We categorized our field site into categories to determine if significant differences existed in snow depth between severely burned forested areas and lower severity burn areas with more intact canopy cover.

In our field site during the 2022 water year, severe wildfire impacts, including the removal of tree canopy structure has increased snow depths in previously unburned, forested areas. We found that reduced interception and mid-winter melt in unburned areas before Mar 21, resulted in enhanced snow depths that persisted until May 1. While our findings appear to be at odds with previous studies of wildfire and snow, they can be explained by differences in climate. Most studies that have investigated the effects of wildfire on snowpacks have been conducted in continental climates with cold winters where shortwave radiation is the dominant term in the energy balance. Our field site is relatively low elevation (~1400 m) and characterized by mild winter air temperatures.

The presence of living trees and associated meteorological conditions including longwave radiation appeared to counteract the well-known effects of increased solar radiation incident to the snow surface and increased albedo in the burned forest, in both second growth and mature forests, resulting in a balance of snow depth loss rate between low, moderate, and high severity burned forest. It is possible that interception related losses and midwinter snowmelt can be the dominant controls on snowpack depths in low to mid-elevation forested areas of the Pacific Northwest.

BIBLIOGRAPHY

Barnett, T. P., Adam, J. C., & Lettenmaier, D. P. (2005). Potential impacts of a warming climate on water availability in snow-dominated regions. *Nature, 438*(7066), 303–309. https://doi.org/10.1038/nature04141

Biederman, J., Brooks, P., Gochis, D., Harpold, A., Gutmann, E., Reed, D., Pendall, E., & Ewers, B. (2014). Multiscale observations of snow accumulation and peak snowpack following widespread, insect-induced lodgepole pine mortality. *Ecohydrology, 7*(1), 150–162. https://doi.org/10.1002/eco.1342

Broxton, P. D., Harpold, A. A., Biederman, J. A., Troch, P. A., Molotch, N. P., & Brooks, P. D. (2015). Quantifying the effects of vegetation structure on snow accumulation and ablation in mixed-conifer forests. *Ecohydrology, 8*(6), 1073–1094. https://doi.org/10.1002/eco.1565

Burles, K. (2010). *Snowmelt energy balance in a burned forest stand, Crowsnest Pass, Alberta* (Master's thesis, University of Lethbridge, Department of Geography). Retrieved from https://opus.uleth.ca/handle/10133/2562

Currier, W. R., & Lundquist, J. D. (2018). Snow depth variability at the forest edge in multiple climates in the Western United States. *Water Resources Research, 54*(11), 8756–8773. https://doi.org/10.1029/2018WR022553

Deems, J. S., Painter, T. H., & Finnegan, D. C. (2013). Lidar measurement of snow depth: A review. *Journal of Glaciology, 59*(215), 467–479. https://doi.org/10.3189/2013JoG12J154

Dharmadasa, V., Kinnard, C., & Baraër, M. (2023). Topographic and vegetation controls of the spatial distribution of snow depth in agro-forested environments by UAV lidar. *The Cryosphere, 17*(3), 1225–1246. https://doi.org/10.5194/tc-17-1225-2023

Dickerson-Lange, S. E., Howe, E. R., Patrick, K., Gersonde, R., & Lundquist, J. D. (2023). Forest gap effects on snow storage in the transitional climate of the Eastern Cascade Range, Washington, United States. *Frontiers in Water, 5*, 1115264. https://doi.org/10.3389/frwa.2023.1115264

Gleason, K. E., McConnell, J. R., Arienzo, M. M., Chellman, N., & Calvin, W. M. (2019). Four-fold increase in solar forcing on snow in western U.S. burned forests since 1999. *Nature Communications, 10*, 2026. https://doi.org/10.1038/s41467-019-09935-y

Gleason, K. E., & Nolin, A. W. (2016). Charred forests accelerate snow albedo decay: Parameterizing the post-fire radiative forcing on snow for three years following fire. *Hydrological Processes, 30*(22), 3855–3870. https://doi.org/10.1002/hyp.10897

Gleason, K. E., Nolin, A. W., & Roth, T. R. (2013). Charred forests increase snowmelt: Effects of burned woody debris and incoming solar radiation on snow ablation. *Geophysical Research Letters, 40*(19), 4654–4661. https://doi.org/10.1002/grl.50896

Harder, P., Pomeroy, J. W., & Helgason, W. D. (2020). Improving sub-canopy snow depth mapping with unmanned aerial vehicles: Lidar versus structure-from-motion techniques. *The Cryosphere, 14*(5), 1919–1935. https://doi.org/10.5194/tc-14-1919-2020

Harder, P., Schirmer, M., Pomeroy, J., & Helgason, W. (2016). Accuracy of snow depth estimation in mountain and prairie environments by an unmanned aerial vehicle. *The Cryosphere, 10*(6), 2559–2571. https://doi.org/10.5194/tc-10-2559-2016

Harpold, A. A., Biederman, J. A., Condon, K., Merino, M., Korgaonkar, Y., Nan, T., Sloat, L. L., Ross, M., & Brooks, P. D. (2014). Changes in snow accumulation and ablation following the Las Conchas Forest Fire, New Mexico, USA. *Ecohydrology, 7*(2), 440–452. https://doi.org/10.1002/eco.1363

Hedstrom, N. R., & Pomeroy, J. W. (1998). Measurements and modelling of snow interception in the boreal forest. *Hydrological Processes, 12*(10-11), 1611–1625. https://doi.org/10.1002/(SICI)1099-1085(199808/09)12:10/11<1611::AID-HYP684>3.0.CO;2-4

Iglesias, V., Balch, J. K., & Travis, W. R. (2022). U.S. fires became larger, more frequent, and more widespread in the 2000s. *Science Advances, 8*(13), eabc0020. https://doi.org/10.1126/sciadv.abc0020

Jacobs, J. M., Hunsaker, A. G., Sullivan, F. B., Palace, M., Burakowski, E. A., Herrick, C., & Cho, E. (2021). Snow depth mapping with unpiloted aerial system lidar observations: A case study in Durham, New Hampshire, United States. *The Cryosphere, 15*(4), 1485–1500. https://doi.org/10.5194/tc-15-1485-2021

Kampf, S. K., McGrath, D., Sears, M. G., Fassnacht, S. R., Kiewiet, L., & Hammond, J. C. (2022). Increasing wildfire impacts on snowpack in the western U.S. *Proceedings of the National Academy of Sciences, 119*(6), e2200333119. https://doi.org/10.1073/pnas.2200333119

Kim, S. (2015). ppcor: An R package for a fast calculation to semi-partial correlation coefficients. *Communications for Statistical Applications and Methods, 22*(6), 665–674. https://doi.org/10.5351/CSAM.2015.22.6.665

Koshkin, A. L., Hatchett, B. J., & Nolin, A. W. (2022). Wildfire impacts on western United States snowpacks. *Frontiers in Water, 4*. https://doi.org/10.3389/frwa.2022.971271

Koutantou, K., Mazzotti, G., Brunner, P., Webster, C., & Jonas, T. (2022). Exploring snow distribution dynamics in steep forested slopes with UAV-borne LiDAR. *Cold Regions Science and Technology, 200*, 103587. https://doi.org/10.1016/j.coldregions.2022.103587

Lawler, R. R., & Link, T. E. (2011). Quantification of incoming all-wave radiation in discontinuous forest canopies with application to snowmelt prediction. *Hydrological Processes, 25*(21), 3322–3331. https://doi.org/10.1002/hyp.8150

Li, D., Wrzesien, M. L., Durand, M., Adam, J., & Lettenmaier, D. P. (2017). How much runoff originates as snow in the western United States, and how will that change in the future? *Geophysical Research Letters, 44*(12), 6163–6172. https://doi.org/10.1002/2017GL073551

Lumbrazo, C., Bennett, A., Currier, W. R., Nijssen, B., & Lundquist, J. (2022). Evaluating multiple canopy-snow unloading parameterizations in SUMMA with time-lapse photography characterized by citizen scientists. *Water Resources Research, 58*(8), e2021WR030852. https://doi.org/10.1029/2021WR030852

Lundquist, J. D., Dickerson-Lange, S. E., Lutz, J. A., & Cristea, N. C. (2013). Lower forest density enhances snow retention in regions with warmer winters: A global framework developed from plot-scale observations and modeling. *Water Resources Research, 49*(9), 6356–6370. https://doi.org/10.1002/wrcr.20504

Malle, J., Rutter, N., Mazzotti, G., & Jonas, T. (2019). Shading by trees and fractional snow cover control the subcanopy radiation budget. *Journal of Geophysical Research: Atmospheres, 124*(6), 3195–3207. https://doi.org/10.1029/2018JD029908

Mankin, J. S., Viviroli, D., Singh, D., Hoekstra, A. Y., & Diffenbaugh, N. S. (2015). The potential for snow to supply human water demand in the present and future. *Environmental Research Letters, 10*(11), 114016. https://doi.org/10.1088/1748-9326/10/11/114016

Marlon, J. R., Bartlein, P. J., Gavin, D. G., Long, C. J., Anderson, R. S., Briles, C. E., Brown, K. J., Colombaroli, D., Hallett, D. J., Power, M. J., Scharf, E. A., & Walsh, M. K. (2012). Long-term perspective on wildfires in the western USA. *Proceedings of the National Academy of Sciences of the United States of America, 109*(9), E535-543. https://doi.org/10.1073/pnas.1112839109

Maxwell, J. D., Call, A., & St. Clair, S. B. (2019). Wildfire and topography impacts on snow accumulation and retention in montane forests. *Forest Ecology and Management, 432*, 256–263. https://doi.org/10.1016/j.foreco.2018.09.021

Mazzotti, G., Currier, W. R., Deems, J. S., Pflug, J. M., Lundquist, J. D., & Jonas, T. (2019). Revisiting snow cover variability and canopy structure within forest stands: Insights from airborne lidar data. *Water Resources Research, 55*(6), 6198–6216. https://doi.org/10.1029/2019WR024898

McGrath, D., Zeller, L., Bonnell, R., Reis, W., Kampf, S., Williams, K., Okal, M., Olsen-Mikitowicz, A., Bump, E., Sears, M., & Rittger, K. (2023). Declines in peak snow water equivalent and elevated snowmelt rates following the 2020 Cameron Peak wildfire in northern Colorado. *Geophysical Research Letters, 50*(4), e2022GL101294. https://doi.org/10.1029/2022GL101294

MTBS. (2022). Burn severity data product. Retrieved from https://mtbs.gov/direct-download

Pomeroy, J., & Schmidt, R. A. (1993). The use of fractal geometry in modelling intercepted snow accumulation and sublimation. *Proceedings of the 50th Eastern Snow Conference*, 1–10.

Reilly, M. J., Zuspan, A., Halofsky, J. S., Raymond, C., McEvoy, A., Dye, A. W., Donato, D. C., Kim, J. B., Potter, B. E., Walker, N., Davis, R. J., Dunn, C. J., Bell, D. M., Gregory, M. J., Johnston, J. D., Harvey, B. J., Halofsky, J. E., ... Kerns, B. K. (2022). Cascadia burning: The historic, but not historically unprecedented, 2020 wildfires in the Pacific Northwest, USA. *Ecosphere, 13*(8), e4070. https://doi.org/10.1002/ecs2.4070

Roth, T. R., & Nolin, A. W. (2017). Forest impacts on snow accumulation and ablation across an elevation gradient in a temperate montane environment. *Hydrology and Earth System Sciences, 21*(11), 5427–5442. https://doi.org/10.5194/hess-21-5427-2017

Rutter, N., Essery, R., Pomeroy, J., Altimir, N., Andreadis, K., Baker, I., Barr, A., Bartlett, P., Boone, A., Deng, H., Douville, H., Dutra, E., Elder, K., Ellis, C., Feng, X., Gelfan, A., Goodbody, A., ... Yamazaki, T. (2009). Evaluation of forest snow processes models (SnowMIP2). *Journal of Geophysical Research: Atmospheres, 114*(D6). https://doi.org/10.1029/2008JD011063

Sicart, J. E., Essery, R. L. H., Pomeroy, J. W., Hardy, J., Link, T., & Marks, D. (2004). A sensitivity study of daytime net radiation during snowmelt to forest canopy and atmospheric conditions. *Journal of Hydrometeorology, 5*(5), 774–784. https://doi.org/10.1175/1525-7541(2004)005<0774

Skidmore, P. B. (1994). *Snow accumulation and ablation under fire-altered lodgepole pine forest canopies* (Master's thesis, Montana State University, Bozeman, MT). Retrieved from Montana State University ScholarWorks

Skiles, M., Flanner, M., Cook, J., Dumont, M., & Painter, T. (2018). Radiative forcing by light-absorbing particles in snow. *Nature Climate Change, 8*(10), 964–971. https://doi.org/10.1038/s41558-018-0296-5

Smoot, E. E., & Gleason, K. E. (2021). Forest fires reduce snow-water storage and advance the timing of snowmelt across the western U.S. *Water, 13*(24), 3533. https://doi.org/10.3390/w13243533

Storck, P., Lettenmaier, D. P., & Bolton, S. M. (2002). Measurement of snow interception and canopy effects on snow accumulation and melt in a mountainous maritime climate, Oregon, United States. *Water Resources Research, 38*(11), 5-1–5-16. https://doi.org/10.1029/2002WR001281

Trujillo, E., Ramirez, J., & Elder, K. (2009). Scaling properties and spatial organization of snow depth fields in sub-alpine forest and alpine tundra. *Hydrological Processes, 23*(11), 1575–1590. https://doi.org/10.1002/hyp.7270

U.S. Forest Service. (2020). *Burned Area Emergency Response Summary – Lionshead Fire*. Willamette, Mt. Hood, and Deschutes National Forests. Retrieved from https://www.fs.usda.gov/Internet/FSE_DOCUMENTS/fseprd835655.pdf

Westerling, A. L., Hidalgo, H. G., Cayan, D. R., & Swetnam, T. W. (2006). Warming and earlier spring increase western U.S. forest wildfire activity. *Science, 313*(5789), 940–943. https://doi.org/10.1126/science.1128834

Winkler, R. D. (2011). Changes in snow accumulation and ablation after a fire in south-central British Columbia. *Streamline Watershed Management Bulletin, 14*(2), 1-7.

Winkler, R. D., Spittlehouse, D. L., & Golding, D. L. (2005). Measured differences in snow accumulation and melt among clearcut, juvenile, and mature forests in southern British Columbia. *Hydrological Processes, 19*(1), 51–62. https://doi.org/10.1002/hyp.5757

Zhao, M., Boll, J., & Brooks, E. S. (2021). Evaluating the effects of timber harvest on hydrologically sensitive areas and hydrologic response. *Journal of Hydrology, 593*, 125805. https://doi.org/10.1016/j.jhydrol.2020.125805